Economic and design optimisation of a 15MW floating offshore wind platform using time-series forecasting

Craig White[1,3], Victor Benifla[2], José Cândido[1], Luís M. C. Gato[3]
[1] WavEC Offshore Renewables, Lisbon, 1350-352, Portugal
[2] University of Rostock, 18051, Rostock, Germany
[3] Instituto Superior Técnico (IST), Lisbon, 1049-001 Portugal

Correspondence to: Craig White(craig.white@wavec.org)

Abstract. A structural and economic optimisation framework applicable to floating semi-submersible platforms, demonstrated here for a 15-MW offshore wind design, is presented. A genetic algorithm was developed that can seek a multi-objective solution to minimise mass whilst respecting the constraints of loads acting upon the system. Statistical and machine learning methods are then employed to forecast near and far term costs of the platform under a range exogenous data scenarios, selected to support and boost forecasting accuracy alongside a hybrid forecasting method. Steel mass was reduced from 3916t to 3273t whilst respecting platform response constraints. The uncertainty of steel prices has the most significant impact on CAPEX, approximately €150-200M at 1GW level. Levelized Cost of Energy (CoE) is calculated to gauge the technical and economic viability, with 3-5€/MWh variation across forecasts.

1 Introduction

The deployment of floating wind turbines (FOWTs) into deeper waters can harness improved wind resources with reduced marine competition and visual impacts. Floating technology has grown rapidly since the first full-scale prototype in 2009 (Skaare, et al., 2015), with pre-commercial status achieved in 2017 (Jacobsen & Godvik, 2021), 50MW in 2021 (Risch, et al., 2023) and 88MW in 2023 (Musial, et al., 2023), but growth has since stagnated. Costs have increased in the recent macroeconomic context and must decrease to achieve commercial gigawatt-level capacities (DNV, 2023). Areas of cost reduction potential should be prioritised including the floating substructure (Barter, et al., 2020). Floating offshore wind (FOW) levelized cost of energy (LCoE) must reduce to compete in auctions against other renewable energy technologies.

This cost problem offers space for innovative solutions across three main platform areas: dimensions, cost and type of materials, and matching the design to site conditions. There are currently four main designs of support structure which are yet to standardise like fixed offshore wind monopiles and jacket foundations. Barges allow concrete construction and can dampen wave action and heave floater motions (Beyer, et al., 2015). Tension-leg platforms (TLPs) transfer loads to the taut mooring and anchoring system, lowering platform mass. Spars are ballast-stabilised and have a simplified cylindrical design and higher draft. Semi-submersibles are buoyancy-stabilised with a wider platform which can operate in shallower waters. High volumes of steel allow for geometry reductions to the structural steel components: namely the inner column, outer columns, pontoons and upper supports. This is true for reference platforms that offer valuable standardised designs for research and technology progression and provide a conservative layout, akin to prototype projects to ensure reliability.

Market prices for key raw materials like steel have witnessed high volatility in recent years, impacting CAPEX and project viability. Methods to accurately predict future prices would reduce risk and improve strategic planning for developers, especially for forecasts accurate initial feasibility to final investment decision (FID) and procurement. Among these, time-series forecasting (TSF) models using statistical and machine-learning methods offer solutions by looking at historical data to make future predictions.

This work implements TSF models to achieve a mass-minimised platform design by predicting commodity prices for the primary steel mass for strategic planning. A structural optimisation will iterate within the design space and defined boundary constraints. The platform structural dynamic response in six degrees of freedom is examined using RAFT (Hall, et al., 2022) to maintain stability under a range of environmental load conditions. Price forecasts will be obtained using TSF models to achieve a mass-optimized platform CAPEX under a range of cost scenarios. The reference IEA 15MW wind turbine (Gaertner, et al., 2020) and UMaine reference Volturn-US-S (V-US) platform (Allen, et al., 2020) are used.

2 Literature review

2.1 Floating platform: design, frequency response, and optimization

2.1.1 Support structure design

The main engineering challenge for FOW maintaining stability in the marine environment whilst generating electricity. Nacelle motion, wave sensitivity and the mooring system footprint are outlined by (Butterfield, et al., 2005) and highlight how these challenges have already been overcome in the oil and gas industry. These challenges necessitated the development of frequency-domain codes that enabled rapid structural assessment across multiple design iterations. They condensed designs into ballast, buoyancy, and tension stabilization, noting that in practice designs are hybrid and an optimal point may lie between each type. Serial production in high volumes and onshore assembly also were found to offer economic benefit. Concept and deployed semi-submersibles alongside numerical simulation tools were reviewed by (Liu, et al., 2016) and confirmed the same design classifications and its design simplicity and maturity justifies its selection in this study.

Due to the complexity and cost of sea testing, numerical modelling such as the frequency-domain codes utilised in this research are preferable for dynamic response studies. The 15MW wind turbine follows other reference designs (Bak, et al., 2013) (Jonkman, et al., 2009) and encompasses a three-bladed rotor, Class IB direct-drive generator, variable-speed and collective pitch controller, a rotor diameter of 240m and a hub height of 150m. The turbine is designed for a fixed monopile foundation but has considerations and applicability for FOW and follows the trend of using fixed offshore wind turbines with thicker towers. The V-US floater (Allen, et al., 2020) is aligned for larger 15MW turbines. A steel platform connects three outer columns and pontoons to a central column that interfaces with the tower. All significant geometric values and coordinates allow design integration within numerical models for analysis, such as those employed in this study.

As turbines increase in size offshore, scaling laws are important to model the impact of larger generators on platform size, with smaller increase in platform size supporting larger generators, improving LCoE. The study by (Papi & Bianchini, 2022) found ballasted mass increased 1.3 times for a tripling of power rating from 5-15MW. The generic upscaling methodology to transfer a FOW turbine geometry from 5MW-15+MW was proposed by (Wu & Kim, 2021), analysing the effects of changes to the column radius and floating base, which are also used in this research. Results showed that upscaling the column radius increased the overall mass and natural heave period, whilst upscaling the column distance raised the centre of gravity and metacentric height of the system, with a slight lowering of the natural heave period that is important for semi-submersible designs. These issues can be minimized through added ballast mass to lower the centre of gravity and increased added mass to raise the natural heave period. Ballast was maintained constant within this study to focus on the impact of structural steel changes.

2.1.2 Numerical models

All structural, aerodynamic and hydrodynamic loads should be considered when modelling the response behaviour of a floating turbine. A study by (Wayman, et al., 2006) investigated joining the structural and aerodynamics of the time-domain FAST with the numerical code of WAMIT for FOW systems in depths ranging from 10-200m. Coupled loads include the gyroscopic motion of the rotor on the system and forces from wave excitation. Modelled motions were found to be acceptable with changing water depth and wind speed.

The FAST model developed by the National Renewable Energy Laboratory (NREL) models the coupled response of floating wind turbines under realistic ocean conditions, validated with the Statoil-Hywind 2.3MW demonstrator FOWT (Driscoll, et al., 2016). With metocean measurements main input variables, the overall response of the platform and loads agreed well with measured data and validated the model's performance for the spar structure. For FOW computationally efficient design optimisation, and utilised in this work, the Response Amplitude of Floating Turbines code (RAFT) looks to the full integrated system (Hall, et al., 2022). Co-design of the support structure, turbine and controller are modelled in the frequency domain for added computational efficiency and design improvements. Three reference FOW designs were modelled and were compared with OpenFAST simulations. The dynamic response spectra and statistics performed well and within an acceptable range that verified the model's application to FOW studies. A review of modelling techniques for floating offshore wind turbines (Otter, et al., 2021) reiterated the challenge of strong coupling of the turbine aerodynamics and platform hydrodynamics. It highlights the move towards high-fidelity modelling due to the cost and complexity of physical testing, although not necessarily with CFD due to long simulation times. The paper concludes that numerical modelling is a trade-off between accuracy and computational efficiency and that many numerical models require improvement, with CFD an option towards the end of the design phase. Physical testing can validate and calibrate numerical models and can be classed into full physical and hybrid testing, with the choice often down to phase, facilities, budget, and test uncertainties. A 3D finite element analysis (FEM) model for FOW support structures (Campos, et al., 2017) argued that common tools ignore the structural stiffness of the elements constituting the floating platform and are normally treated as rigid body. Flexibility was found to be crucial in structural lifetime analysis and this paper proposes a model to integrate the deformation of the structure within a fully coupled hydro-aero-servo-elastic time domain model. In the study presented here, computational efficiency is critical and a flexible-body finite element model is not the main focus. Multiple designs variants and load cases that impact the overall platform dynamics and system response would make a detailed structural assessment unfeasible at this stage.

2.1.3 Design optimization

The design optimization solves for an objective function such as platform mass by adjusting geometrical parameters whilst adhering to specified constraints. A complex reliability-based framework of a spar-type FOW support structure (Mareike & Kolios, 2021) coupled economic efficiency with design uncertainties. Environmental conditions, limits and uncertainties were specified and a reliability assessment defined which generated a response surface for various system geometries. The method met all constraints including the reliability criteria and reduced platform and ballast mass. A software framework for a 22 MW Semisubmersible FOW platform (Zalkind & Bortolotti, 2024) was developed for the matching reference wind turbine. Various fidelity levels and load cases were evaluated for controller adjustment, plus the difference between sequential and simultaneous co-design. An algorithm that searches the design space before optimisation is suggested, and that solving smaller problems sequentially is advantageous rather than large simultaneous co-design solutions. Notwithstanding a more robust and reliable outcome, the simultaneous solution was found to produce a platform with 2% lower mass and therefore a trade-off between advantageous results and reliability is required. The current research also features a sequential optimisation for design, system load response, and economic analysis and similar system mass reduction results. An efficient optimisation tool for floating offshore wind support structures (Faraggiana, et al., 2022) highlights the need for economic competitiveness through a reduction of the platform weight and therefore structural cost, matching the objectives of this paper with the same optimisation method albeit for a different platform. An optimisation tool applicable to any floating turbine is proposed that adjusts the geometry, in this case the OC3 spar-type design. The stability and dynamic performance were evaluated and optimised using a genetic algorithm (GA) coupled with a surrogate model to both minimise cost and maximise performance. Cost reductions across the best and worst cases of 2-3 times were found, with a 25% cost decrease between most and least restrictive optimal cases. Hydrostatic constraints were found to be more significant than dynamic ones due to influencing the design area.

The genetic algorithm is a useful tool which simulates natural reproduction and the fitness of certain populations to combine attributes and produce better offspring which help to achieve the objective function, allowing multi-objective analysis and design space visualisation. This makes GA’s ideal for optimizing complex systems, such as FOW substructure designs, where optimisation involves different design variables, complex numerical models and non-linear constraints and reinforces the choice of optimization method in this study, involving multiple designs and load cases within a constrained optimization.

A global optimisation tool identified and evaluated the configuration of support structures for FOW (Hall & Buckham, 2012). The rationale highlighted the nascent stage of FOW optimisation and the complex nature of FOW system interactions in multiple mediums that inhibit the convergence of designs. Also, geometrical optimisation has previously omitted key design parameters which drives the need for a flexible GA approach. Results show designs similar in nature to established spar and semi-submersible configurations, with others less conventional, and lead to the selection of the RAFT tool used within this work. A GA framework was developed (Hall, et al., 2013) to optimize the support structure for FOW using a nine-variable parameterization, which is equal to the method employed in the current research. This broadened the design space further than the state of art that considered a frequency-domain dynamics model linearized forces that recreated the physical considerations acting on the turbine and support structure whilst remaining computationally efficient. The choice of GA allowed a visualisation of the design space and pareto front that showed optimal design choices, through minimization of both the support structure cost and root-mean-squared (RMSE) nacelle acceleration

2.2 Economic analysis: Costs, LCoE, and forecasting methods

2.2.1 Costs and LCoE

Feasibility of FOW (Musial, et al., 2004) showed a technical description of several floating platforms classed by mooring system, especially between contrasting catenary and taut vertical systems. A cost comparison was made between a semi-submersible and an NREL TLP, both supporting a 5MW turbine. Production costs for the semi-submersible reduced by 40% under structural optimisation. Such reductions build the case for structural optimisation and its impact on LCoE. Lifecycle LCoE perspective by (Myhr, et al., 2014) provided a detailed cost assessment of the main discussed structures. Mass-based calculations utilised in this research were derived alongside the cost of mooring and anchoring systems, with depth and distance to shore found to drive LCoE. High economic variability was found of designs, and the potential for cost reduction. Further work recommended progression of cost calculations to include scale effects for mass-produced components and tailoring components and system design to site conditions, reflected in this research through varying load conditions.

A systems engineering vision for FOW optimisation (Barter, et al., 2020) identified gaps to reduce the CoE, mainly through a system-integrated approach to capture complex interactions and physics across the lifecycle of a FOW farm. A range of cost-reduction research areas were outlined including new hybrid substructures, anchoring methods, two-bladed and/or downwind rotors, alternative materials and FOW-specific controls. These cost-reductions are realised through a combination of Economy of Scale (EoS) effects, improved learning rates and design optimisation through research. FOW high potential areas were defined by (James & Ros, 2015), with the floating platform highest with a 16% reduction in CAPEX from prototype to commercial scale, again reinforcing the focus on platform optimization.

2.2.2 Timeseries forecasting

Forecasting of time-series data, observations made sequentially though time, is crucial in the areas of science, industry, commerce and economics (Chatfield, 2020). It can consist of forecasting just one time-series, or a group of either separate forecasts or grouped data which supports one forecast, as presented here. A variety of predictive regressive models can perform this task, with machine learning models able to capture complex patterns, and statistical models capturing seasonal and longer-term trends. A seasonal autoregressive model with exogenous variables (SARIMAX) model forecasted short-term electricity load in (Tarsitano & Amerise, 2017) which managed accurate predictions through dynamic regression, for a shorter timeframe of multiple days. Residuals de-trend the data and were supported by exog hourly loads and calendar effects. An eXtreme Gradient Boosting algorithm (XGBoost) used by (Zhang, et al., 2023) predicted energy and peak power for 1-3 years. Multi-step forecasting which includes recursive and sequential training, was employed to measure accuracy and stability. Hybrid combinations of these models, capture the benefits of each to produce accurate future predictions, as utilised in this work.

The platform's steel shell costs are susceptible to market prices of primary and secondary steel, which have been highly variable in recent years (Albulescu, 2021) and especially after a global pandemic. Forecasts must be statistically sound and predicted with highest possible confidence. For specific commodity price forecasts, there is already research within statistics, machine learning, deep learning and neural networks that have already been applied to the platform materials studied in this work, namely steel. A method by (Wang, et al., 2020) into neural networks used a long short-term memory with exog features, with success in predicting trends over recurrent neural networks. The one-dimensional time series was restacked to enable period correction of seasonal features, by calculating and grouping data residuals as employed in the SARIMAX forecasts in this work.

Steel prices were forecasted by (Jin & Xu, 2024) using gaussian process regressions. The model was trained using cross-validation and Bayesian optimizations, resulting in a low root mean square error (RMSE) of 0.54% between 2019 and 2021. Due to the structured data of most time series, machine learning and statistical models usually outperform more complex methods over longer timeframes, with both methods used within this research. Accurate time-series forecasting could help inform procurement strategies, auction bids, and aid investor confidence with lower risk. But care must be taken in model accuracy to ensure they are robust and to prevent access to actual data in the predictions during testing. This research has not been thoroughly applied within the context of steel for floating wind and presents a promising study area to explore.

3 Method

This work can be divided into two main areas: First, the platform mass minimization that is a combination of RAFT and a GA, which delivers a minimized mass that satisfies the overall constraints of the simulation. Second, the economic assessment that costs the floater based on forecasts of structural marine steel. Generalised project costs and power generation are then used to calculate the final LCoE over a range of future years to help strategize future floating offshore wind procurement.

3.1 Model for platform response and design optimization

The design of the V-US platform is composed of one central and three outer columns linked through pontoons and upper supports. Here, the design variables are continuous real values and defined as the main platform diameter (D), the centre and outer columns diameters (d_{cc}, d_{oc}), and the height, width and thickness of the pontoon (h_{po}, w_{po}, t_{po}), with parametrization highlighted in . Any other design parameters for the substructure, mooring system, or turbine remain fixed with values from the base model.

The objective of this design optimisation problem is to minimize the total mass while ensuring its dynamic performance. The FOWT system is evaluated in terms of dynamic responses under a reduced set of load cases. While the environmental conditions in this study are not site-specific, they were selected based on experience values and previous design optimisation studies (Dou, et al., 2020) to represent typical conditions that need to be assessed for the development of FOWT substructures according to standards. Typically, these must include the rated wind speed of the rotor and harsh sea states to represent worst cases scenarios. Additionally, the three representative environmental conditions are chosen to reflect typical values for rated mean wind speed and sea state encountered in Europe, as seen in (Messmer, et al., 2023). It is also worth noting that there is no wind-wave misalignment and that the mean wind force is normal to the rotor plane.

Table 1 - Load conditions for design optimisation

	Units	LC 1	LC 2	LC 3	LC4	LC5	LC 6
Wind speed	Ws (m.s-1)	11	19	23	3	7	70
Sig. wave height	Hs (m)	1.10	2.04	2.85	6.3	8.0	10.68
Sig. wave period	Tp (s)	7.19	8.11	8.82	11.50	12.70	14.20
Operation state				Operating			Parked
Closest comparison with IEC DLCs	1.2	1.2	1.2	1.1/1.2	1.1/1.2	1.1/1.2	6.1

In this design optimisation study, the dynamic performance of the FOWT system is evaluated with constraints on specific aspects of the platform response and turbine behaviour. The maximum platform offset, the platform pitch, and the nacelle acceleration at the top of the tower in the wind direction are constrained ensuring these values remain within acceptable limits. Finally, the fore-aft bending moment at the tower base and the static stress at the location at the interface between the central column and the pontoons are also considered and limited as they represent the stress that can be transferred to the substructure and is commonly limited in design. Each of these constraints values are computed for each defined load case and the maximum result across all cases is selected to be checked against the constraint limits of the optimisation problem. Defining these constraint limits to accurately represent real-world conditions can be challenging, so they are often set to general values based on experience. This approach is also applied here, supported by insights from previous optimisation and simulation studies and other publicly available models of the V-US.

The main inputs for the design optimisation study presented here are gathered and summarized in . Due to the inherent randomness of GA's the design optimisation problem is run 10 times to collect statistical results from multiple optimisation runs and properly assess the results and efficiency. For each run, the population starts at 100 individuals and the maximum number of generations is capped at 1000 for a reasonable amount of evaluation for this large design space.

3.1.1 Platform response

The main objective is the mass minimisation of a 15-MW semi-submersible platform. The design optimisation framework presented in (Benifla & Adam, 2023) was applied to the V-US substructure mounted with the IEA 15-MW reference offshore wind turbine (Gaertner, et al., 2020). In this study, the Response Amplitude of Floating Turbines (RAFT) open-source code is used to model the FOWT system in the frequency-domain and evaluate its static properties and dynamic response. The code has been validated against higher-fidelity tools such as OpenFAST and has shown good agreement while also being computationally efficient. This makes it an ideal choice for quickly evaluating various substructure designs under different environmental conditions (Hall, 2022).

In RAFT, the FOWT system is modelled as a rigid body with the common six degrees of freedom: surge, sway, heave, roll, pitch, and yaw. The dynamics are represented in the frequency domain, allowing the FOWT system to respond linearly to each excitation frequency. The complex amplitude of the system's response, X, at a given frequency ω, is obtained by solving the generic equation of motion for the FOWT system:

$$(-\omega^2 M + i\omega B + K)X(\omega) = F_{ext}(\omega), \qquad (1)$$

where, M, B, and K represent the FOWT system's total mass, damping, and stiffness matrices, respectively, F_{ext} the external excitation forces, and ω the frequency. The frequency-domain dynamics of the FOWT are assumed to operate around a specific position, $\overline{X}$, which represents the mean steady state of the system. This position is obtained by solving iteratively the static equilibrium equation derived from the previous equation:

$$K_h = \overline{F}_{ext} + \overline{F}_{moor}\overline{(X)}, \qquad (2)$$

where $\overline{F}_{ext}$ represents the mean external forces applied to the system, $\overline{F}_{moor}$ is the nonlinear reaction force of the mooring system (the effective mooring stiffness), and K_h is the total hydrostatic stiffness.

In RAFT, the system can be evaluated under given environmental conditions defined by steady winds and stochastic sea states, characterized by a mean wind speed Ws and a JONSWAP wave spectrum with significant wave height Hs and peak period Tp. The rotor-nacelle assembly is modelled as a rigid body with three identical blades and specific dimensions (chord, twist angle, and prebend) and distributed aerodynamic properties (lift and drag coefficients). The tower is defined as a cylindrical member, and the floating substructure as a combination of interconnected members of different shapes, with mass, inertia, buoyancy, and hydrostatic stiffness obtained by summing individual contributions. Mean aerodynamic loads are computed using a steady-state blade-element momentum solver, while mooring forces are determined with a quasi-static solver. Stochastic events including turbulent wind fields, gusts, and extreme waves are of importance to aerodynamic and hydrodynamic loads acting on the system but are time-domain phenomena, incompatible to the frequency domain RAFT tool employed and the large number of design iterations and integration with the GA. The system's fast frequency response is obtained by linearizing the dynamic equations, accounting for rotor aerodynamics and hydrodynamic damping based on Morison's equation applied to discretized substructure strips. Finaly, RAFT computes the FOWT's mean offset and frequency-domain response, with maximum values estimated by combining the mean values and the complex response spectra. The maximum platform offset and other key quantities of interest—such as the tower-top nacelle acceleration and the tower-base bending moment in the fore-aft can be obtained. Different design load cases can be defined to include multiple wind and wave conditions, enabling a comprehensive evaluation of the system's dynamic response under various environmental scenarios.

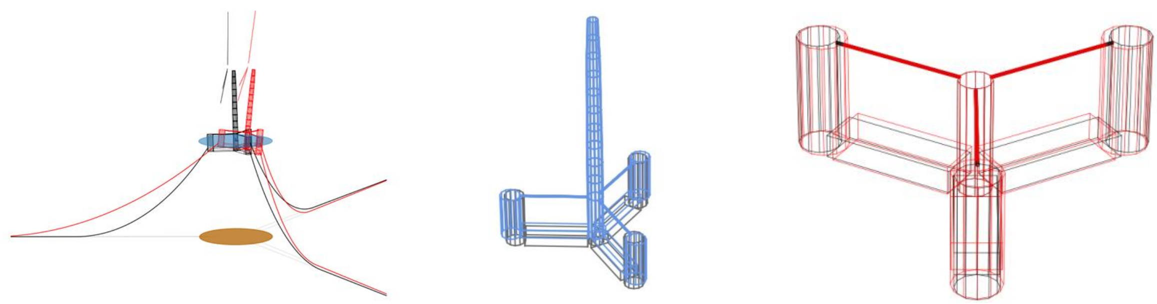

Figure 1. a) RAFT model of the floating wind turbine in static position and maximum offset, b) Optimal system including tower, and c) Optimised semi-submersible platform design

A static stress analysis is performed to assess the structural integrity of potential designs. In this analysis the focus is at the interface between the central column and pontoon. To estimate the loads, a free-body approach is followed, where the contributions of both the outer column and the pontoon itself are considered. Only considered here are structure weight and the buoyancy loads inducing moments on the structure interface. The stress σ on the pontoon base is:

$$\sigma = M \, {}^{h_{po}}\!\big/_{(2 \cdot I_{po})}, \tag{3}$$

where M is the total bending moment, and h_{po} and I_{po} are the height and second moment of area of the pontoon section.

3.1.2 Design optimization

The main objective is to reduce the steel mass of the V-US platform under several constraints to account for the dynamic of the system. For a given design solution, represented by x, the constrained single-objective optimisation problem can be:

Minimize:

$$m(x)$$

Subject to:

$$\begin{aligned} X_{Li} \le X_i \le X_{Ui} \quad & i = 1, \dots, n_x \\ g_j(X) \le g_{jlim} \quad & j = 1, \dots, n_g \end{aligned}, \tag{4}$$

where m is the steel mass, X_{Li} and X_{Ui} denote the lower and upper limits of the design space and g_j is an inequality constraint with its associated limit g_{jlim}. These constraints are typically the output of the numerical analysis previously described that are monitored and constrained.

To solve, an efficient GA is implemented and inspired by (Hall, 2013). This was applied to FOWT substructure design, and addresses limitations of traditional evolutionary algorithms by identifying local optima and avoiding unnecessary problem evaluations. A distance-weighted scaling operation is performed to ensure that each local optimum identified within the population are treated equally. Throughout the optimisation, the fitness of the entire population is scaled, leading to the total scaled population fitness as described in (Hall, 2012). This is combined with a constraint-handling technique used by (Deb, 2000) allowing infeasible solutions to be compared solely based on their total constraint violation. This form of the penalty enables a clear comparison between feasible and infeasible solutions, allowing the GA to handle constraints effectively.

The initial population is generated and evolves by using Simulated Binary Crossover (SBX) and a polynomial mutation operation, originally introduced in (Deb & Agrawal, 1995). These efficient operators are widely used addressing real-valued optimisation problems. After new offspring are generated, they are assessed before being added to the current population. This ensures that they not too alike existing individuals while remaining close to fit ones. The check avoids the computational cost of evaluating the problem for individuals not added. This approach is particularly beneficial here, as evaluating the objective and constraint functions requires significant computational resources to run the numerical models described. It also ensures that the population evolves toward fitter regions of the design space, resulting in lower population density in less fit areas. The structure of the framework is shown in Fig. 2 and illustrates the interaction between the GA and the RAFT dynamic model.

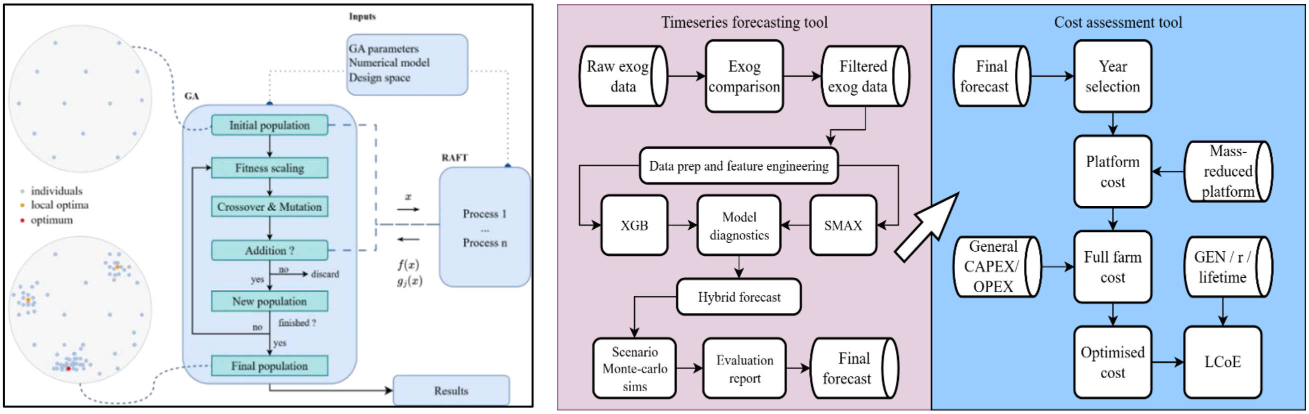

Figure 2. Process flow of a) Design optimisation and b) Timeseries forecasting and cost assessment tool

3.2 Time series forecasting and economic assessment

After the design optimisation of the platform, an economic assessment is applied to the optimal platform, and reference design. A range of future costs up to seven years ahead are forecasted using a combination of forecasting methods. Second, these costs are applied to the final structure to derive a cost at platform and farm level, alongside an LCoE assessment.

3.2.1 Timeseries forecasting

The price forecasting tool incorporates a combination of models: a short-term XGB which captures stochastics and fluctuation well, and a statistical SARIMAX model better at capturing seasonality and long-term trends. The best performing singular or hybrid version was selected based on rolling hindcast testing windows. Both models rely on exog data that are provided in the form of monthly prices, indices and other economic metrics. These supporting data are monthly time series of equal shape and granularity to the target predictor (HRC steel prices). They are external to the steel prices themselves but are linked (such as metals with impact on steel, metal indexes, energy prices, among others) which allow the predictor to build confidence. For. The equation the XGB total objective function $L\phi$ is:

$$L\phi = \sum_{i=1}^{n} I(y_i, \hat{y}_i) + \sum_{k=1}^{K} \Omega(f_k) \, , \tag{5}$$

where $I(y_i, \hat{y}_i)$ the loss function between measured and predicted values, $\Omega(f_k)$ the regularization term which s complexity to reduce overfitting, f_k the $k\text{-}th$ weakest decision tree learner in the group, and k the total number of decision trees.

For the SARIMAX model, finding the future steel price y_t when applied to a differenced stationary dataset is:

$$y_t = \mu + \phi(B)\Phi(B^S)(1-B)^d(1-B^S)^D y_t + \theta(B)\Theta(B^S)\varepsilon_t + \beta X_t, \tag{6}$$

with μ the mean level of series, B the backshift operator defining the lags, for non-seasonal $(1-B)^d$ and seasonal $(1-B^S)^D$ differencing, $\phi(B)$ the nonseasonal and $\Phi(B^S)$ the seasonal autoregressive terms, $\theta(B)$ the non-seasonal and $\Theta(B^S)$ the seasonal moving average, ε_t the error term and βX_t the exog variables. The SARIMAX model simultaneously models the temporal behaviour of the steel prices and the influence of the selected external (exog) economic variables, allowing the prediction to be influenced by external market conditions and not just the past influence of steel prices.

Candidate exogs $x_{t,}$ with the top-ranking group shown in **Error! Reference source not found.** are compared to the target steel prices $y_{t,}$ and filtered using statistical comparison metrics r (7), with monthly lag testing b (8) and rolling stability (9):

$$r(\Delta\log x_{t,}\Delta\log y_{t,}), \tag{7}$$

$$r(\Delta\log x_{t-b,}\Delta\log y_{t,}), \tag{8}$$

$$r_{t} = corr(\Delta\log x_{t,}\Delta\log y_t)_{rolling}, \tag{9}$$

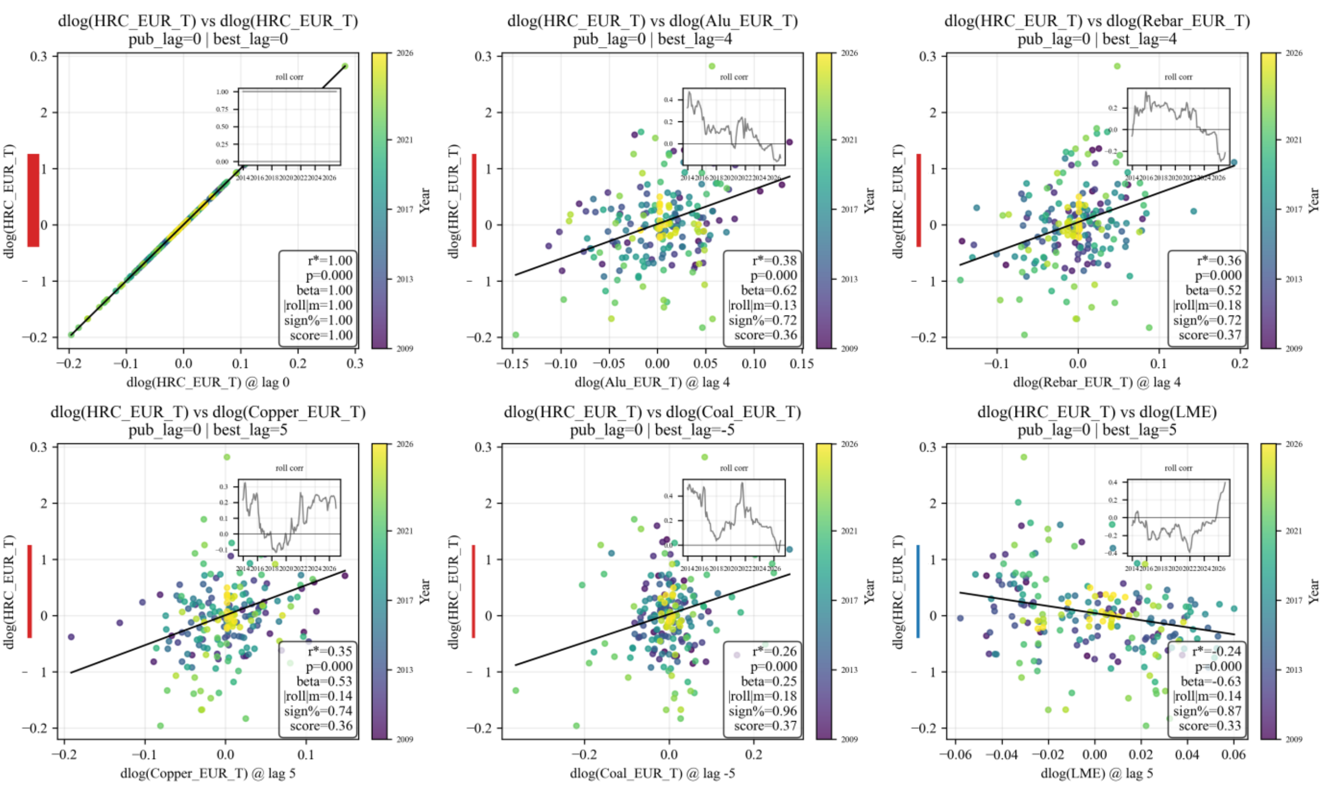

Figure 3. Comparison of best performing exogenous data and target steel predictor data

The best performing exog datasets are collected which pass multiple checks including stability, sign, mean strength, and lags, to create an optimum set of suitable supporting data for the forecasts and are shown in Fig. 3. The x-axis shows the publication delay applied to the variable (months), and the y-axis the memory length (how many observations retained in the model). Red and blue bars positive or negative trends, and thicker bars representing better performance. Multiple transformations (level, first difference, log-difference), lags and lengths are tested. Each exog receives a score based on the predictive strength, stability magnitude, and sign consistency. Only those that pass all thresholds and highest-ranked are stored in the final data group to boost prediction accuracy. Examples of the exog data passing the cross-correlation analysis with the target steel price are; rebar and copper acting as leading indicators; coal; London Metal Exchange LME). Such indicators are robust for inclusion into future steel forecasting.

The next phase transforms the exog data into $x_{t,}$ $\log x_{t,}$ and $\Delta \log x_{t,}$, then detrended with residuals where required, then ranked for usefulness, stability, and non-redundancy. Features including $\Delta\log(y_{t-1})$, $\Delta\log(y_{t-12})$, x_{t-b}, and x_{t-b-k} are then added, with b, k the best delay and memory term respectively, for the target $\Delta\log(y_{t,})$. The hybrid forecast $\hat{y}_{hy}$ combines the XGB and SARIMAX forecasts with two formulations: A weighted linear combination (10) with w the weight assigned to XGB, and a horizon-based regime switching method (11) with H the threshold horizon separating long and short term (3, 6, … months) h the forecast horizon in months:

$$\hat{y}_{hy\,=}\, w\hat{y}_{XGB} + (1-w)\hat{y}_{SAR}, \tag{10}$$

or

$$\hat{y}_{hy\,=} = \begin{cases} \hat{y}_{XGB}, & h \leq H_{short} \\ \hat{y}_{SAR}, & x > H_{long} \end{cases}, \tag{11}$$

The final model is evaluated based on RMSE, mean absolute percentage error (MAPE) and symmetric mean absolute percentage error (sMAPE).

3.2.2 Economic assessment

The forecast monthly steel prices are first aggregated into yearly values $P_{y,s}^{HRC}$ and converted to marine grade steel for platform cost analysis, found from (BVG, 2025). Only the primary steel mass is impacted by the price forecasts in this study, which forms almost the entire cost. Steel is assumed to be purchased in a given year where contracts with the fabricator are agreed, it is not assumed that all units are purchased in that year.

$$P_{y,s}^{HRC} = \frac{1}{n_y}\sum_m \hat{P}_{m,s}^{HRC}, \tag{12}$$

With $P_{m,s}^{HRC}$ the monthly predicted values, n_y the number of monthly observations and s the forecast scenario. Other platform components including secondary steel items, ballast and controls are costed from literature as other CAPEX, as they are not the main subject of this study and primary steel contributes around 83% of the total platform (BVG, 2025). The platform cost $CAPEX_{plat}$ can be found by:

$$CAPEX_{plat} = P_{y,s}^{marine} \cdot M_d \cdot N_p \tag{13}$$

With $P_{y,s}^{marine}$ the price of marine grade steel, M_d the mass of platform design and N_p the number of platforms, omitted for one platform. Total CAPEX is the summation of the platform CAPEX and all other CAPEX. Other wind farm costs are generalised from (BVG, 2025) to remove site-specific and project bias, with primary steel mass of the platform removed to allow space for the optimised platform. A net capacity factor of 0.4925 that considers all losses including electrical are used for a floating offshore 1GW wind farm (Beiter, et al., 2020), validated with a gross CF of 0.5024 (Martini, et al., 2016) to arrive at an LCoE value per year of the forecast. LCoE is then placed within the current framework of to see how both the economic and structural design optimisation influence both platform cost and $LCoE$:

$$LCoE_{y,s,d}^{€/MWh} = \frac{CAPEX_{y,s,d}^{total} + PV_{OPEX} PV_{DECEX}}{PV_E} \tag{14}$$

With $CAPEX_{y,s,d}^{total}$ the total CAPEX for year y, PV_{OPEX}, PV_{DECEX}, and PV_E the present value of OPEX, DECEX, and energy generation respectively, discounted to present.

4 Results

4.1 Platform design

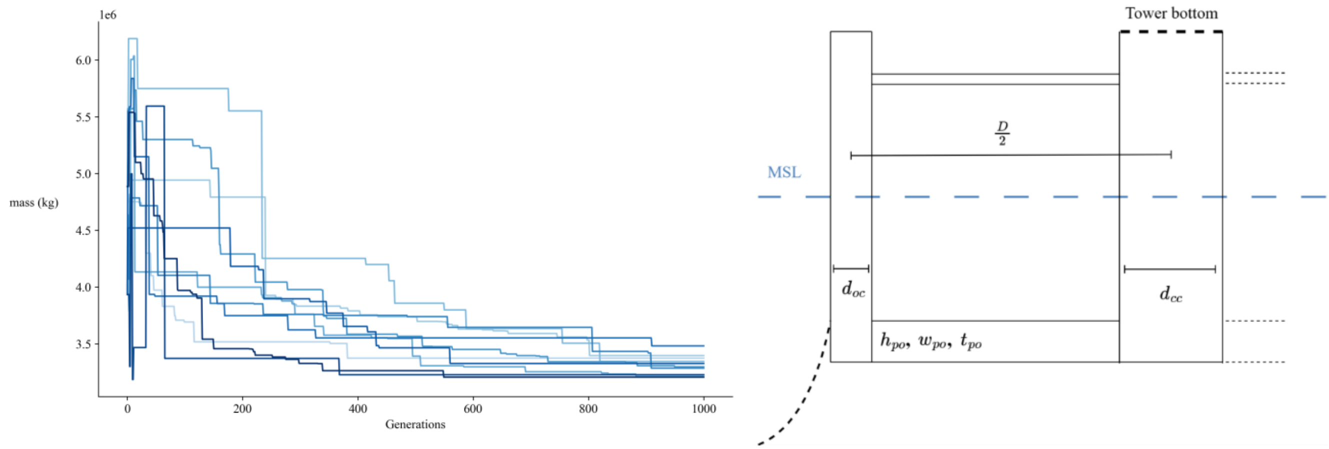

Figure 4. a) Mass/objective evolution for multiple runs b) Cross section of substructure and design parameters

The steel mass evolution of the best individual in the population through its evolution for all the runs is presented in Fig. 4. This shows the algorithm's performance in minimizing the objective while reaching feasible regions of the design space where constraints are respected. The statistical results collected from the 10 optimisation runs showed consistent performance, with small standard deviations and some small variation between run outputs. These results also shows that the algorithm led to near optimal solutions in some runs highlighting the importance of repeated optimisation. Out of all the runs, the chosen optimized design is gathered and compared with the base model shown in Fig. 1 (black base, optimised red and blue) and the following Table 2. The worst successful design is chosen for the rest of this work so that it constitutes a safety margin that encapsulate some of the aspect neglected here. As expected, the mass is minimized while keeping the dynamic behaviour of the system as well as its structural integrity. The optimized mass obtained can be considered quite low when compared to the original, but this is anticipated as the structural check of potential designs is relatively simple here and lacks more in-depth analysis of the structure behaviour in terms of dynamic stress analysis. Mainly the optimized design exhibit slightly larger outer columns and pontoon dimensions but with a smaller platform diameter. Indeed, the design optimisation work presented here allows for a first optimized design that can be considered in the subsequent economic analysis. For further detailed analysis, once could consider other environmental analysis design space and enhance structural analysis to reach more confidence in the final optimize design.

Table 2 – Main characteristics of platform design and loads

Parameter	Units	Limits	Original	Optimised	% reduction
Diameter	m	[50, 150]	103.5	108.8	5%
Draft	m	[15, 40]	20	15	-25%
Diameter outer col	m	[10, 30]	12.5	13.1	5%
Height pontoon	m	[5, 20]	7.00	5.56	-21%
Width pontoon	m	[5, 20]	12.40	8.66	-30%
Shell mass	t		3916	3273	-16%
Platform offset	m	<25	23.16	24.82	7%

Pitch	º	<5	5.70	4.98	-13%
Nacelle acceleration	m/s²	<3m	1.76	1.78	1%
Stress	Mpa	<300	161.8	205.0	27%

4.2 Timeseries forecasting

The XGB, SARIMAX, and hybrid forecasts are shown in Fig. 5 for the model tested on hindcast data, running sequentially for 3-year phases. Model performance over the testing period 2022-2024, a period of high market fluctuation, improves with both hybrid forecasts and with the addition of exog data. Without supporting exog data to boost the prediction accuracy, the predicted values remain above actual prices and do not revert to the mean, with the price floor now raised due to the observed price spike in 2020 and cannot be considered a reliable baseline forecast. With exog supporting data, the SARIMAX forecast is continual decay in response to the 2022 price drop, showing a negative systematic price prediction bias. The hybrid model, selecting the best option for each predictor step, also adds accuracy to the model. The best performing exog supporting data (including other metals, indexes, and indicators, collected into the greatest hits collection of supporting data) produces the best testing results of 187.5 Mean Averaged Error (MAE) and shows the model's improvements when adding support and blended forecasting, and present a suitable candidate for future baseline scenarios.

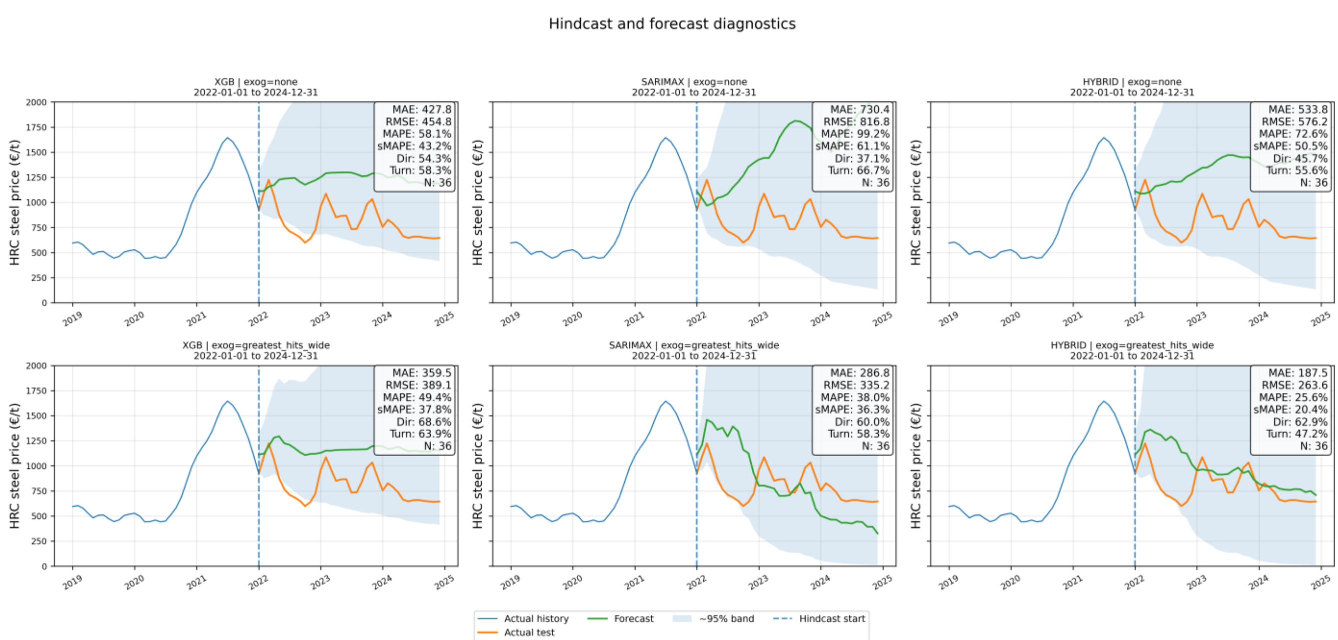

Figure 5. Hindcast diagnostics of real and forecasted data for varying models and exogenous supporting data

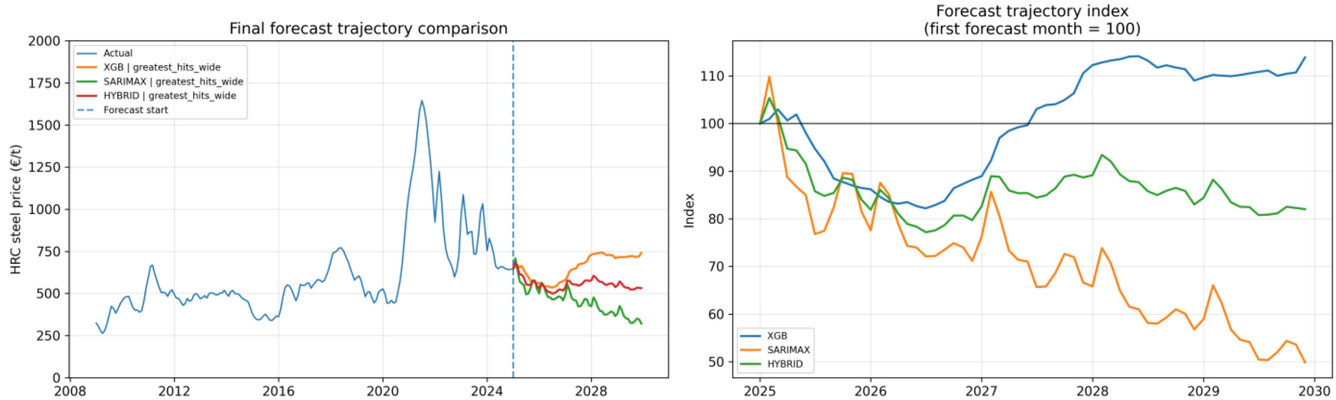

Figure 6. Short to long-term forecasts of HRC steel prices using XGB, SARIMAX and hybrid forecasts

The future predictions ahead of current data after hindcast testing are presented in Fig. 6. The XGB forecast recovers prices after an initial drop and can be considered a market recovery scenario, with a rebound of 10-15% showing no continual drift. The SARIMAX forecast up until the end of 2029 shows continual downwards drift which could be due to a lack of data transformation before forecasting. The hybrid forecast, alongside the best exog collection provides a balanced path and a moderate forecast which would be suitable for baseline projections, with the other two models providing upper and lower bounds.

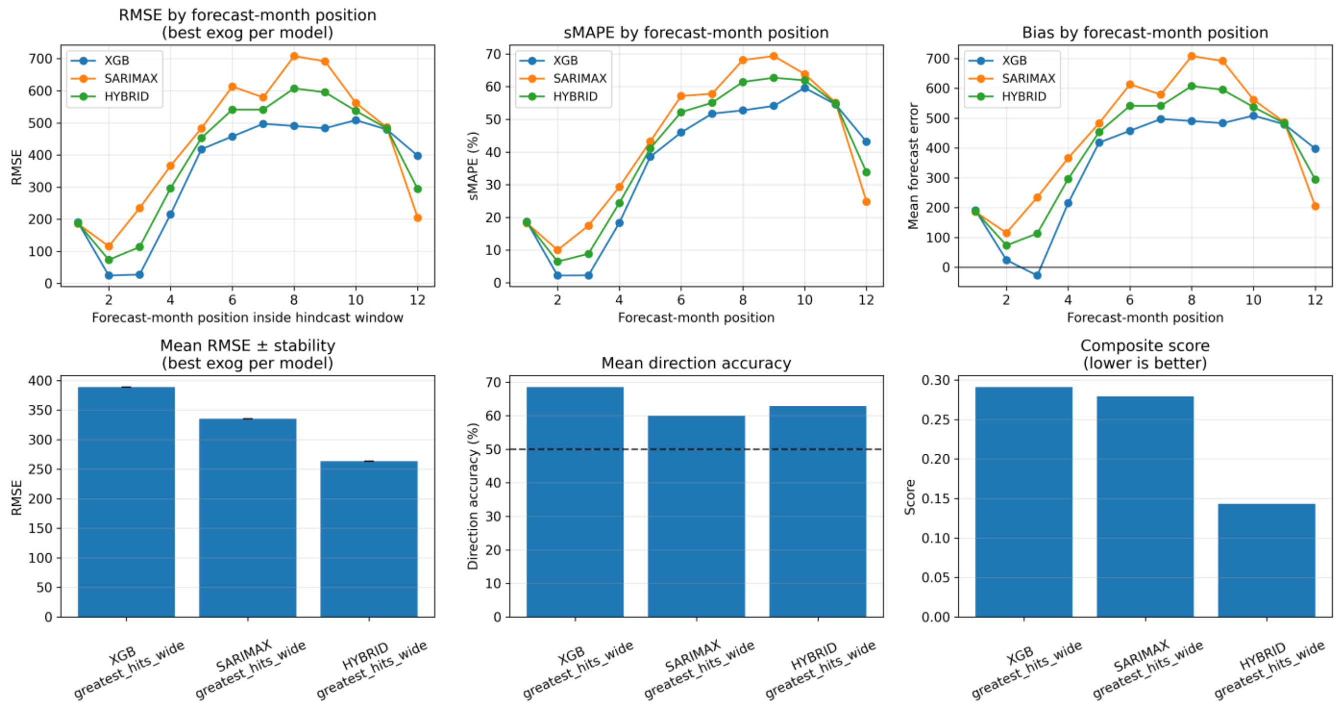

Figure 7. Forecast month analysis and model performance

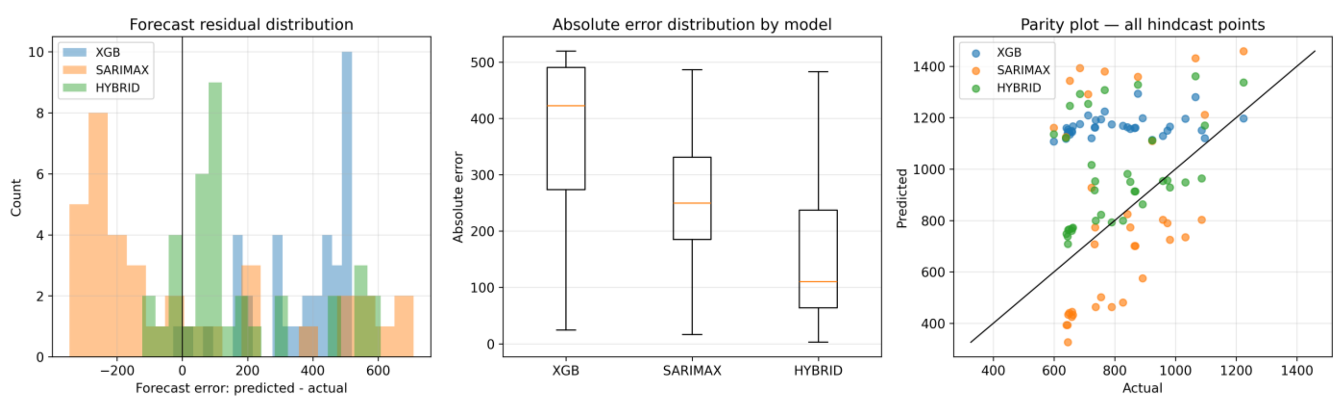

Figure 8. Diagnostic analysis of XGB and SARIMAX forecasts

The error structure by month position is shown in Fig. 7 and shows all models as expected worsen with horizon, especially the SARIMAX forecast with a large spike in RMSE, symmetrical mean absolute percentage error (sMAPE), and mean forecast error. sMAPE measures the average relative difference between observed and forecasting values, treating over and under-prediction equally. The XGB has higher overall stability but still performs worse than the hybrid forecast, which produce the lowest MAE during the hindcast test period and held relatively low root-mean-squared-error (RMSE) and sMAPE, with a mean bias (or average forecast error) close to zero. It provided the most consistent performance across the defined metrics Interestingly and unexpectedly, SARIMAX performs best in the short-term and seems errors rise with the negative forecast bias. However, this could be due to more data preparation or transformation. An evaluation of the XGB, SARIMAX, and hybrid models against the actual hindcast data can be seen in Fig. 8. In support of the hindcasts testing results, the hybrid model again proves most valuable, with lower forecast errors, error and a tighter spread of data points closer to actual results, with residuals centred around zero. The XGB has a positive bias through overestimation from, with the SARIMAX the opposite with a tendency for underprediction.

4.3 Economic assessment

The steel price and LCoE with changing forecast year are shown below in Fig. 9 , for the three scenarios and for the two types of platform: Initial mass of 3916t and optimised 3273t, around 10-15% savings across scenarios and which is the best and consistent outcome from the GA model. With the predictions affecting only steel prices, the CAPEX trends follow the same path as in the forecasting results, With XBG and SARIMAX the high and low bounds forecasts, and hybrid the baseline scenario. The uncertainty of steel prices has a significant impact on CAPEX, approximately €150-200M at 1GW level, or by up to 40-50% variation across the range of forecasts. Based on these results, market factors are a primary driver of economic uncertainties, with engineering optimisation offering significant yet partial mitigation.

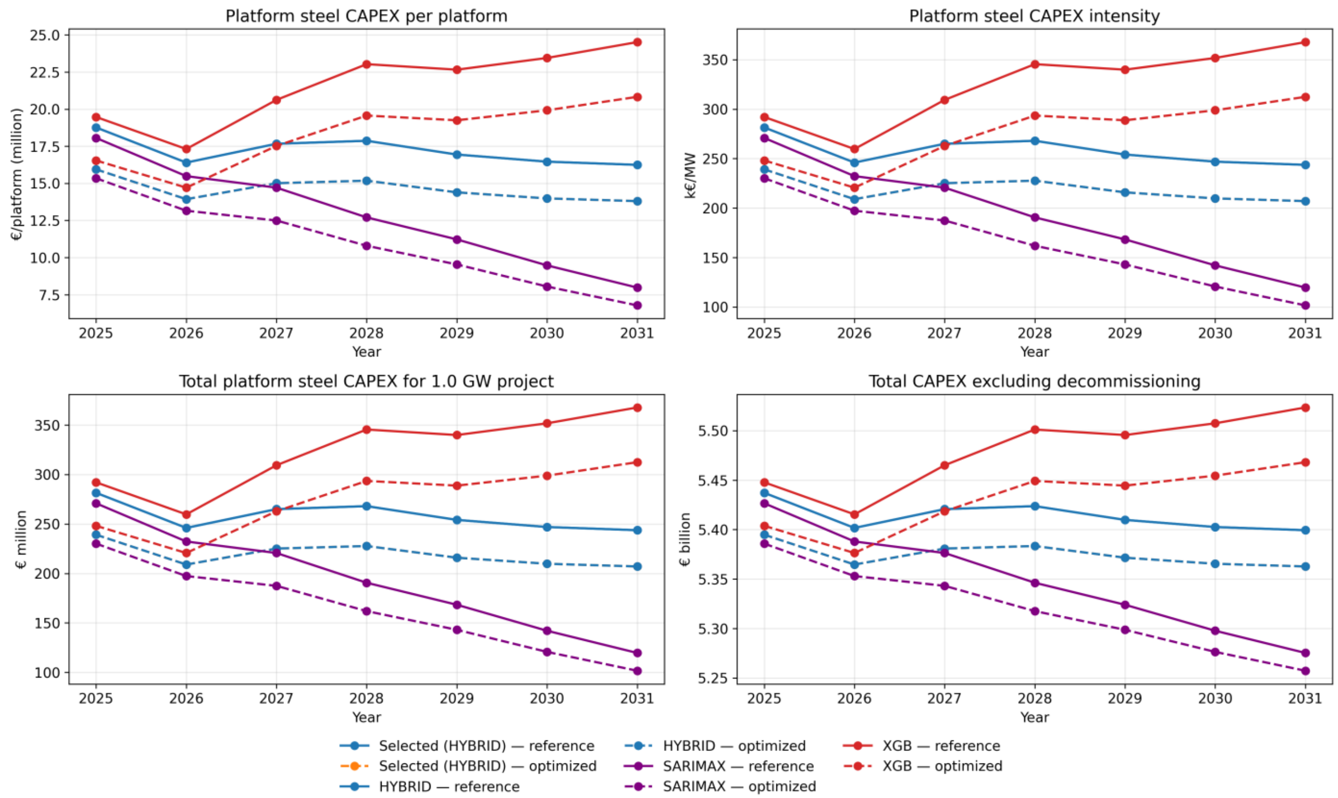

Figure 9. Total cost per platform, per project and for total CAPEX

For LCoE as shown in Fig. 10 shows a more moderate impact, around 3-5€/MWh with effects lessened through a long project lifetime of 30 years and higher discount rates of 8% to reflect early commercial FOW projects, with structural optimization reducing LCoE by around 1€/MWh and more significant in the high-price scenarios. LCoE values are also encompassing other CAPEX items, energy generation, and OPEX, which were all generalised in this work.

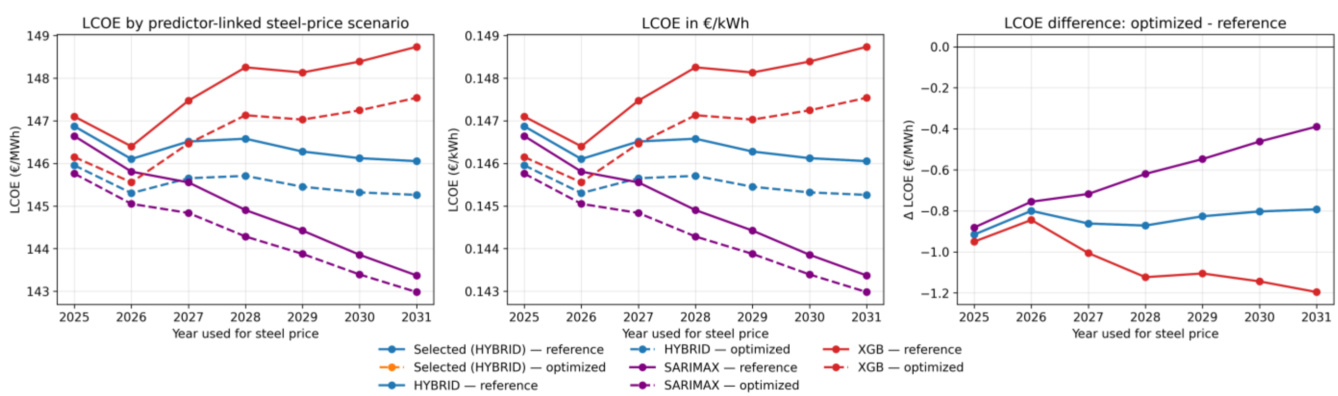

Figure 10. LCoE analysis of the three models and optimized and non-optimized systems

5 Conclusions

This work presented the combination of a platform design optimisation whilst respecting design constraints, and a techno-economic assessment that calculated the platform and project CAPEX using a combination of forecasting methods. The LCoE was estimated using general costs and energy generation from wider literature, which placed the system within both a 1GW farm scale and within the current LCoE framework. Results show that design improvements are possible for the reference platform whilst still respecting the constraints of expected loads acting on the floating turbine in the offshore environment, with savings of 10-15% in steel shell mass.

For cost forecasting, it is possible to blend forecasts to take advantage of the benefits of short-term models that can capture stochastic fluctuation, longer-term statistical models that can capture deeper trends in time-series data. In this research the hybrid model outperformed XGB and SARIMAX model by capturing the benefits of both and combined they form three scenario forecasts. As SARIMAX conversely performed best in early forecast months, more calibration is required to build confidence in future predictions. This work highlights the promising nature of predictive models, especially with selection of supporting data through filtering and wider economic analysis. Overall, the market fluctuations are strong drivers of platform CAPEX with €150-200M at 1GW level, or 40-50% fluctuation across all scenarios, and 3-5€/MWh LCoE. This shows economic forces are strong drivers of CAPEX and LCoE for a high priority cost reduction area for floating offshore wind. These, alongside the benefit of design optimization measures, must reduce for commercial potential to be realised.

6 Data availability

The RAFT code is available at https://github.com/NLRWindSystems/RAFT (last access: 27 July 2026), The RAFT methodology and implementation are described by Hall et al. (2022), https://doi.org/10.1088/1742-6596/2265/4/042020. The genetic algorithm used for the design optimisation is available at https://github.com/vbenifla/VikOpti/tree/main. Code for timeseries forecaster is available at https://doi.org/10.5281/zenodo.21631992

7 Author contributions

Economic analysis and time series forecasting code development and writing by Craig White. Platform design optimisation, simulations, development of genetic algorithm and writing by Victor Benifla. Results and manuscript review by José Cândido. Assistance with submission and support by Luís M. C. Gato.

8 Competing interests

The contact author has declared that none of the authors has any competing interests.

9 References

Albulescu, C. T.: COVID-19 and the United States financial markets' volatility, Finance Res. Lett., 38, 101699, https://doi.org/10.1016/j.frl.2020.101699, 2021.

Allen, C., Viselli, A., Dagher, H., Goupee, A., Gaertner, E., Abbas, N., Hall, M., and Barter, G.: Definition of the UMaine VolturnUS-S reference platform developed for the IEA Wind 15-megawatt offshore reference wind turbine, National Renewable Energy Laboratory, Golden, CO, USA, NREL/TP-5000-76773, https://doi.org/10.2172/1660012, 2020.

Bak, C., Zahle, F., Bitsche, R., Kim, T., Yde, A., Henriksen, L. C., Natarajan, A., and Hansen, M. H.: Description of the DTU 10 MW reference wind turbine, DTU Wind Energy, Roskilde, Denmark, DTU Wind Energy Report-I-0092, 2013.

Barter, G. E., Robertson, A., and Musial, W.: A systems engineering vision for floating offshore wind cost optimization, Renew. Energy Focus, 34, 1–16, https://doi.org/10.1016/j.ref.2020.03.002, 2020.

Beiter, P., Musial, W., Duffy, P., Cooperman, A., Shields, M., Heimiller, D., and Optis, M.: The cost of floating offshore wind energy in California between 2019 and 2032, National Renewable Energy Laboratory, Golden, CO, USA, NREL/TP-5000-77384, https://doi.org/10.2172/1710181, 2020.

Benifla, V. and Adam, F.: Design optimization of floating offshore wind turbine substructure using frequency domain modelling and genetic algorithm, J. Phys.: Conf. Ser., 2626, 012047, https://doi.org/10.1088/1742-6596/2626/1/012047, 2023.

Beyer, F., Choisnet, T., Kretschmer, M., and Cheng, P. W.: Coupled MBS-CFD simulation of the IDEOL floating offshore wind turbine foundation compared to wave tank model test data, in: Proceedings of the 25th International Ocean and Polar Engineering Conference, Kona, Hawaii, USA, 21–26 June 2015, International Society of Offshore and Polar Engineers, 2015.

Butterfield, S., Musial, W., and Jonkman, J.: Engineering challenges for floating offshore wind turbines, in: Proceedings of the Copenhagen Offshore Wind Conference, Copenhagen, Denmark, 26–28 October 2005, National Renewable Energy Laboratory, NREL/CP-500-38776, 2005.

BVG Associates: Guide to a floating offshore wind farm, BVG Associates, Swindon, UK, 2025.

Campos, A., Molins, C., Trubat, P., and Alarcón, D.: A 3D FEM model for floating wind turbines support structures, Energy Procedia, 137, 177–185, https://doi.org/10.1016/j.egypro.2017.10.344, 2017.

Chatfield, C.: Time-Series Forecasting, Chapman and Hall/CRC, https://doi.org/10.1201/9781420036206, 2000.

Deb, K.: An efficient constraint handling method for genetic algorithms, Comput. Method. Appl. M., 186, 311–338, https://doi.org/10.1016/S0045-7825(99)00389-8, 2000.

Deb, K. and Agrawal, R. B.: Simulated binary crossover for continuous search space, Complex Syst., 9, 115–148, 1995.

DNV: Energy Transition Outlook 2023, DNV, Høvik, Norway, 2023.

Dou, S., Pegalajar-Jurado, A., Wang, S., Bredmose, H., and Stolpe, M.: Optimization of floating wind turbine support structures using frequency-domain analysis and analytical gradients, J. Phys.: Conf. Ser., 1618, 042028, https://doi.org/10.1088/1742-6596/1618/4/042028, 2020.

Driscoll, F., Jonkman, J., Robertson, A., Sirnivas, S., Skaare, B., and Nielsen, F. G.: Validation of a FAST model of the Statoil-Hywind Demo floating wind turbine, Energy Procedia, 94, 3–19, https://doi.org/10.1016/j.egypro.2016.09.181, 2016.

Faraggiana, E., Sirigu, M., Ghigo, A., Bracco, G., and Mattiazzo, G.: An efficient optimisation tool for floating offshore wind support structures, Energy Rep., 8, 9104–9118, https://doi.org/10.1016/j.egyr.2022.07.036, 2022.

Gaertner, E., Rinker, J., Sethuraman, L., Zahle, F., Anderson, B., Barter, G., Abbas, N., Meng, F., Bortolotti, P., Skrzypinski, W., Scott, G., Feil, R., Bredmose, H., Dykes, K., Shields, M., Allen, C., and Viselli, A.: Definition of the IEA Wind 15-megawatt offshore reference wind turbine, National Renewable Energy Laboratory, Golden, CO, USA, NREL/TP-5000-75698, https://doi.org/10.2172/1603478, 2020.

Hall, M.: A cumulative multi-niching genetic algorithm for multimodal function optimization, International Journal of Advanced Research in Artificial Intelligence, 1, 6–13, https://doi.org/10.14569/IJARAI.2012.010902, 2012.

Hall, M., Buckham, B., and Crawford, C.: A genetic algorithm-based platform optimization framework for floating offshore wind turbines, in: Proceedings of the 11th International Conference on Sustainable Energy Technologies (SET-2012), Vancouver, Canada, 2–5 September 2012, 2012.

Hall, M., Buckham, B., and Crawford, C.: Evolving offshore wind: A genetic algorithm-based support structure optimization framework for floating wind turbines, in: OCEANS 2013 MTS/IEEE Bergen, Bergen, Norway, 10–14 June 2013, 1–10, https://doi.org/10.1109/OCEANS-Bergen.2013.6608173, 2013.

Hall, M., Housner, S., Zalkind, D., Bortolotti, P., Ogden, D., and Barter, G.: An open-source frequency-domain model for floating wind turbine design optimization, J. Phys.: Conf. Ser., 2265, 042020, https://doi.org/10.1088/1742-6596/2265/4/042020, 2022.

Jacobsen, A. and Godvik, M.: Influence of wakes and atmospheric stability on the floater responses of the Hywind Scotland wind turbines, Wind Energy, 24, 149–161, https://doi.org/10.1002/we.2563, 2021.

James, R. and Costa Ros, M.: Floating offshore wind: Market and technology review, The Carbon Trust, London, UK, 2015.

Jin, B. and Xu, X.: Predictions of steel price indices through machine learning for the regional northeast Chinese market, Neural Comput. Appl., 36, 20863–20882, https://doi.org/10.1007/s00521-024-10270-7, 2024.

Jonkman, J., Butterfield, S., Musial, W., and Scott, G.: Definition of a 5-MW reference wind turbine for offshore system development, National Renewable Energy Laboratory, Golden, CO, USA, NREL/TP-500-38060, https://doi.org/10.2172/947422, 2009.

Katoch, S., Chauhan, S. S., and Kumar, V.: A review on genetic algorithm: Past, present, and future, Multimed. Tools Appl., 80, 8091–8126, https://doi.org/10.1007/s11042-020-10139-6, 2021.

Leimeister, M. and Kolios, A.: Reliability-based design optimization of a spar-type floating offshore wind turbine support structure, Reliab. Eng. Syst. Saf., 213, 107666, https://doi.org/10.1016/j.ress.2021.107666, 2021.

Liu, Y., Li, S., Yi, Q., and Chen, D.: Developments in semi-submersible floating foundations supporting wind turbines: A comprehensive review, Renew. Sust. Energ. Rev., 60, 433–449, https://doi.org/10.1016/j.rser.2016.01.109, 2016.

Martini, M., Guanche, R., Armesto, J. A., Losada, I. J., and Vidal, C.: Met-ocean conditions influence on floating offshore wind farms power production, Wind Energy, 19, 399–420, https://doi.org/10.1002/we.1840, 2016.

Martins, J. R. R. A. and Ning, A.: Engineering Design Optimization, Cambridge University Press, Cambridge, UK, https://doi.org/10.1017/9781108980647, 2022.

Messmer, T., Ran, X., Benifla, V., Lutz, M., Adam, F., Bachynski-Polić, E. E., and Hölling, M.: Overview of the potential of floating wind in Europe based on met-ocean data derived from the ERA5-dataset, J. Phys.: Conf. Ser., 2626, 012021, https://doi.org/10.1088/1742-6596/2626/1/012021, 2023.

Musial, W., Butterfield, S., and Boone, A.: Feasibility of floating platform systems for wind turbines, in: Proceedings of the 42nd AIAA Aerospace Sciences Meeting and Exhibit, Reno, Nevada, USA, 5–8 January 2004, https://doi.org/10.2514/6.2004-1007, 2004.

Musial, W., Spitsen, P., Duffy, P., Beiter, P., Shields, M., Mulas Hernando, D., Hammond, R., Marquis, M., King, J., and Sathish, S.: Offshore Wind Market Report: 2023 Edition, National Renewable Energy Laboratory, Golden, CO, USA, NREL/TP-5000-87232, DOE/GO-102023-6059, https://doi.org/10.2172/2001112, 2023.

Myhr, A., Bjerkseter, C., Ågotnes, A., and Nygaard, T. A.: Levelized cost of energy for offshore floating wind turbines in a life cycle perspective, Renew. Energy, 66, 714–728, https://doi.org/10.1016/j.renene.2014.01.017, 2014.

Otter, A., Murphy, J., Pakrashi, V., Robertson, A., and Desmond, C.: A review of modelling techniques for floating offshore wind turbines, Wind Energy, 25, 831–857, https://doi.org/10.1002/we.2701, 2022.

Papi, F. and Bianchini, A.: Technical challenges in floating offshore wind turbine upscaling: A critical analysis based on the NREL 5 MW and IEA 15 MW reference turbines, Renew. Sust. Energ. Rev., 162, 112489, https://doi.org/10.1016/j.rser.2022.112489, 2022.

Qiu, W., Song, X., Shi, K., Zhang, X., Yuan, Z., and You, Y.: Multi-objective optimization of semi-submersible platforms using particle swam optimization algorithm based on surrogate model, Ocean Eng., 178, 388–409, https://doi.org/10.1016/j.oceaneng.2019.02.039, 2019.

Risch, D., Favill, G., Marmo, B., van Geel, N., Benjamins, S., Thompson, P., Wittich, A., and Wilson, B.: Characterisation of underwater operational noise of two types of floating offshore wind turbines, Scottish Association for Marine Science, Oban, UK, 2023.

Sergiienko, N. Y., da Silva, L. S. P., Bachynski-Polić, E. E., Cazzolato, B. S., Arjomandi, M., and Ding, B.: Review of scaling laws applied to floating offshore wind turbines, Renew. Sust. Energ. Rev., 162, 112477, https://doi.org/10.1016/j.rser.2022.112477, 2022.

Skaare, B., Hanson, T. D., Nielsen, F. G., Yttervik, R., Hansen, A. M., Thomsen, K., and Larsen, T. J.: Analysis of measurements and simulations from the Hywind Demo floating wind turbine, Wind Energy, 18, 1105–1122, https://doi.org/10.1002/we.1750, 2015.

Tarsitano, A. and Amerise, I. L.: Short-term load forecasting using a two-stage SARIMAX model, Energy, 133, 108–114, https://doi.org/10.1016/j.energy.2017.05.126, 2017.

Wang, T., Leung, H., Zhao, J., and Wang, W.: Multiseries featural LSTM for partial periodic time-series prediction: A case study for steel industry, IEEE T. Instrum. Meas., 69, 5994–6003, https://doi.org/10.1109/TIM.2020.2967247, 2020.

Wayman, E. N., Sclavounos, P. D., Butterfield, S., Jonkman, J., and Musial, W.: Coupled dynamic modeling of floating wind turbine systems, in: Proceedings of the Offshore Technology Conference, Houston, Texas, USA, 1–4 May 2006, OTC-18287-MS, https://doi.org/10.4043/18287-MS, 2006.

Wu, J. and Kim, M.-H.: Generic upscaling methodology of a floating offshore wind turbine, Energies, 14, 8490, https://doi.org/10.3390/en14248490, 2021.

Zalkind, D. and Bortolotti, P.: Control co-design studies for a 22 MW semisubmersible floating wind turbine platform, J. Phys.: Conf. Ser., 2767, 082020, https://doi.org/10.1088/1742-6596/2767/8/082020, 2024.

Zhang, T., Zhang, X., Rubasinghe, O., Liu, Y., Chow, Y., Iu, H. H.-C., and Fernando, T.: Long-term energy and peak power demand forecasting based on Sequential-XGBoost, IEEE T. Power Syst., 39, 3088–3104, https://doi.org/10.1109/TPWRS.2023.3289400, 2024.